

## Vortex flow analysis of a large segmented solid rocket motor

Prahalad N. Tengli<sup>1</sup>, C.S. Ramesh<sup>2</sup>, K. Viswanathan<sup>3</sup> and R. Saravanan<sup>4</sup>

<sup>1</sup>Mechanical Engg. Deptt., Dr.M.G.R.Educational & Research Institute University, Chennai-600095, India

<sup>2</sup>Mechanical Engg. Deptt., PES Institute of Technology, Bangalore-560085, India

<sup>3</sup>VAST, SHAR, ISRO, (Retd.)India, <sup>4</sup>R&D Division, SF Complex, DRDO, Jagdalpur-494001, India  
ptengli@yahoo.com, csr\_gce@yahoo.co.in, vmhkv@hotmail.com, smrskv@gmail.com.

### Abstract

It is not uncommon to find pressure oscillations in large size segmented solid rocket motors. During the static test of segmented solid rocket motor (SRM-3), unanticipated pressure oscillations were seen after some of the propellant has burnt and the oscillations sustained for certain duration of time. The purpose of this paper is to present the results of the analysis carried out on the experimental data using commercial CFD software 'FLUENT' and compare the results with experimental data to find out the cause of the pressure oscillations. Inhibitors are provided for the full web thickness of propellant at the segment joint interfaces to prevent end-burning of propellant at the joints. The char and erosion rate of these inhibitors are lower than the burning rate of the propellant. As burning of the propellant progresses, annular inhibition wall starts projecting above the burning surface of the propellant. These obstacles (inhibition) are acting as wall and sheared gas flow occurs in the rocket motor. CFD analysis was carried out on a quadrilateral mesh for the geometry of SRM-3 at the time of 32 s after ignition when the pressure oscillations peaked. It has been found that the vortex shedding frequency obtained by CFD analysis closely matches with the frequency of pressure oscillations occurring during static testing. Thus, it has been revealed that the obstacle vortex shedding generated by the compartmentalization of the combustion chamber by the protrusion of inhibition at the segment joints was the cause of the pressure oscillations in SRM-3.

**Keywords:** Vortex shedding, Segmented Solid Rocket Motor, CFD analysis, Propellant, Combustion chamber

### Introduction

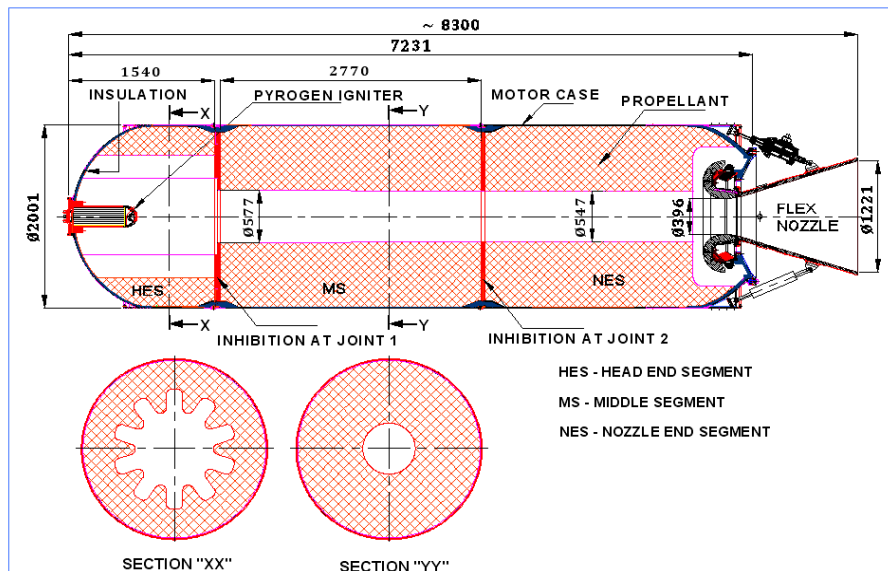
Static test of a large size segmented Solid Rocket Motor called SRM-3 has been carried out as part of the qualification programme. The elements of the SRM-3 are shown in Fig.1.

During the test, unanticipated small amplitude oscillations were observed for certain duration in the Pressure - Time response of the motor (Static Test Report, SFC, 2005). On analysis of data, the frequency of

pressure oscillations was found to be 55.17 Hz (Frequency Analysis Report, SFC, 2006). The amplitude of oscillations was peaking at the time of  $t_0+32$  s;  $t_0$  being the time of ignition of the motor.

Large size solid rocket motors- particularly segmented ones exhibit pressure oscillations during static tests and flight tests. Low frequency (10 to 100 Hz) pressure oscillations may occur due to Characteristic Length ( $L^*$ ) of the motor or due to longitudinal mode acoustic instability (Price, 1977). Based on the geometry of SRM-3, the fundamental acoustic mode in the longitudinal direction should be about 76 Hz which is higher than the observed frequency of 55.17 Hz. Hence, these oscillations might not have occurred due to acoustic instability. Pressure oscillations may also occur due to vortex shedding caused by obstacles in-between the segments of the rocket motor. SRM-3 made of three segments namely head end, middle and nozzle end. Inhibitors are provided for the full web thickness of propellant at these segment joint interfaces to prevent end burning of propellant at the joints. The char and erosion rate of these inhibitors are lower than the burning rate of the propellant. Therefore, as the burning of the propellant progresses, annular inhibition wall projecting above the

Fig.1. Elements of Segmented SRM-3



burning surface of the propellant is formed. These obstacles (inhibition) act as barriers and sheared gas flow result in the rocket motor (Brown *et al.*, 1988). These sheared gas flow is named as obstacle vortex shedding which has been formed due to vortices. It is believed that the highest oscillation amplitudes occur when vortex shedding frequency coincide with the motor longitudinal acoustic mode (Tom Nesman *et al.*, 1996).

Pressure oscillations have been observed in Space Shuttle Re-designed Solid Rocket Motor, Titan IV Solid Rocket Motor Upgrade (Dotson *et al.*, 1997) and Ariane 5 Solid Booster P230 (Scippa *et al.*, 1994). Vortex shedding as a source of pressure oscillations has been analyzed by many researchers. Numerical methods were used successfully to analyze the pressure oscillations in 1/15<sup>th</sup> scale model of Ariane P230 (Yves Fabignon *et al.*, 2003) and full scale P230 Solid Rocket Motor (Stella *et al.*, 2005).

The main objective of this paper is to simulate the conditions of SRM-3 at the time of occurrence of maximum pressure oscillations (32 s after ignition), analyze for vortex shedding using numerical techniques and find out whether the observed pressure oscillation is caused by the obstacle vortex shedding.

**Mathematical formulation**

The commercial CFD code FLUENT has been successfully used for applications related to solid rocket motors (Tom Nesman *et al.*, 1996). The same CFD software was used to study the pressure oscillations in SRM-3. FLUENT uses a control-volume based technique for discretization and numerical solution of field equations. This approach has the coupled solution method that solves the governing equations of continuity, momentum, energy and species transport simultaneously. Because the governing equations are non-linear and coupled, several iterations of the solution loop has been performed to arrive at the converged solution. The Roe-FDS algorithm with courant number, second order upwind has been used to achieve the solver parameters. An implicit discretization of time derivatives has been chosen. The Sutherland viscosity law is involved with three point coefficient method in this model (Fluent Documentation, 2006).

The formula follows:

$$\mu = \mu_o \left( \frac{T}{T_o} \right)^{3/2} \frac{T_o + S}{T + S}$$

$\mu$  = Viscosity in kgf/m-s.

$T$  = Static temperature in ° Kelvin.

$\mu_o$  = Reference value in kgf/m-s.

$T_o$  = Reference temperature in ° Kelvin.

$S$  = Effective temperature in ° Kelvin.

(Sutherland constant)

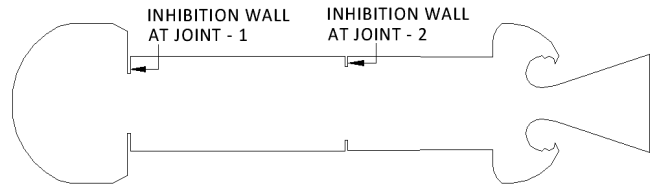
**Geometrical details**

The geometry of SRM-3 at the time of  $t_0+32$  seconds ( $t_0$  being ignition time of the motor) when peak oscillation occurred was considered for analysis. Two inhibition regions (obstacle walls) were considered in the model -

one at the head end segment joint (Joint-1) and the other at the nozzle end segment joint (Joint-2). Overview of the inhibition projections from the propellant surface at the time of  $t_0+32$  s is shown in Fig.2.

Inhibition projection at the head end joint was higher

Fig.2. Overview of burning geometry at  $t_0 + 32$  s



than the projection at the nozzle joint because of higher thickness of inhibition at the head end joint. Also as the expected velocity of gas at the head end region is always less as compared to the velocity at nozzle end joint region, the erosion rate of head end joint inhibition was low. Accordingly, post-test inspection of the SRM-3 revealed larger projection of left-out inhibition at the head end joint compared to the nozzle end joint (Post Test Inspection Report, SFC, 2005).

Knowing the propellant initial web thickness and the total burn time, the surface of the propellant from the axis of the SRM-3 at  $t_0+32$  s was determined. The values of inhibition projection from propellant surface at  $t_0+32$  seconds were arrived at based on left-out inhibition after the test at the respective joints and assuming linear erosion of inhibition for the entire duration of burning. The

Fig.3a. Mesh near obstacle (head end)

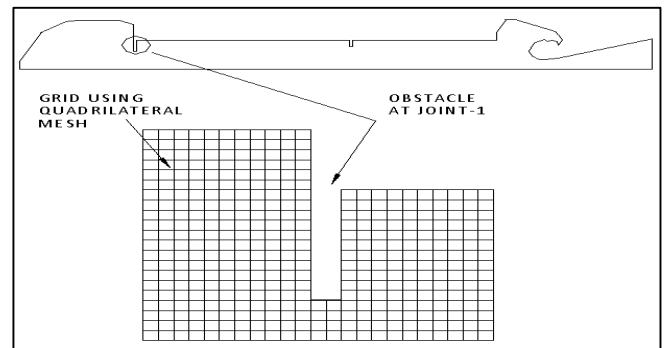
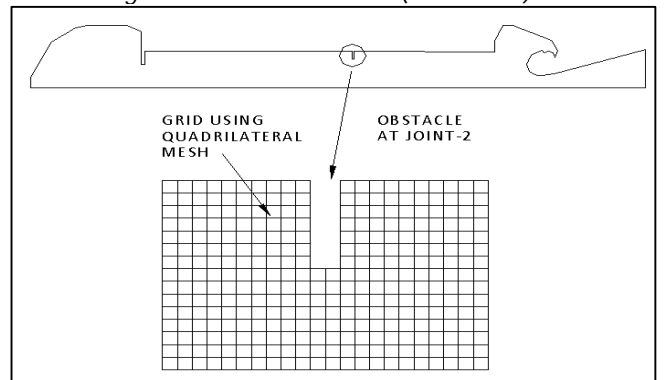


Fig.3b. Mesh near obstacle (nozzle end)



amount of inhibition projection from the propellant surface at  $t_0+32$  s was determined as 194.56mm at the head end joint and 109.17mm at the nozzle end joint.

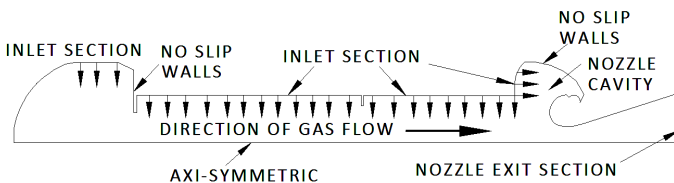
All other relevant geometrical dimensions of SRM-3 have been considered. Inhibition has been considered as wall for the analysis (Stella & Paglia 2009; Abdul Raheem *et al.*, 2004).

Quadrilateral mesh has been implemented. The configuration of burning motor at  $t_0+32$  s has 187404 cells with mesh interval size of 5mm. Fig.3a represents the magnified view of mesh details near inhibition (obstacle) at the head end joint (Joint-1). Fig.3b depicts the magnified view of mesh details of inhibition obstacle at the nozzle end joint (Joint-2). Grid has been done with quadrilateral mesh at an interval of 5mm for better accuracy of results.

**Boundary conditions of the model**

Various assumptions have been made for propellant characteristics and dimensional profile at the time of peak oscillations. The fluid flow was assumed to be in the axial direction toward the SRM-3 nozzle. For this model, inlet conditions were imposed normal to the side walls simulating as inlet in solid propellant combustion (David R Greatrix, 2008). Inhibition and outer surface of nozzle cavity dome were assumed to be walls. The Inlet section has mass flux and 48 bar ( $48 \times 10^5$  Pa) as Gauge pressure at the time of  $t_0+32$ s and Exit section has atmospheric pressure of 1 bar ( $1 \times 10^5$  Pa). Axisymmetric solver was used for the model. The boundary conditions are depicted in Fig.4.

Fig.4. Boundary conditions involved in numerical simulation



**Data Monitored Using Fluent Software**

Due to complexity of the phenomenon under study, a long initial transient has been simulated. After this initial transient, the data acquisition has started. Due to complex oscillatory behavior of the flow, data monitoring conducted for a longer time has been used during processing of data.

The Pressure component has been acquired at control point placed in computational domain. For pressure component, a sampling point (P1) has been chosen near the head end dome as per monitoring location used during static test firing (Test plan, ASL, 2005). This

Fig.5. Sampling point (P1)

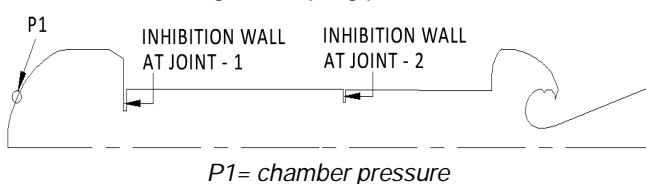


Fig.6. Vortex shedding in Segmented Solid Rocket Motor (SRM-3)

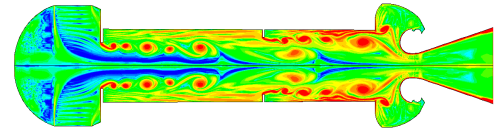
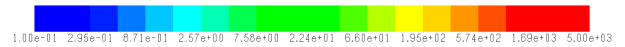
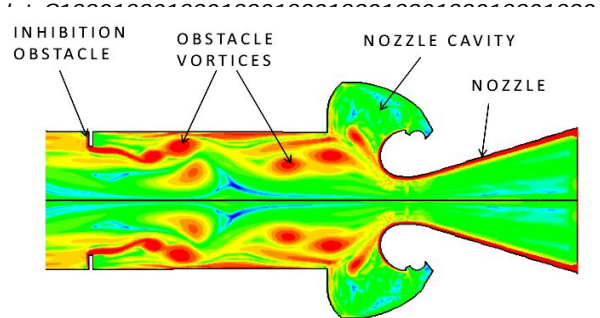


Fig.7. Details of Obstacle



location is shown in Fig.5. The sampling frequency of the numerical solution was 100 kHz and simulations of the statistically stationary phase have been carried out nearly four seconds of physical time.

The study of the frequency response of the pressure oscillation data was based on a spectral analysis conducted by means of Fast Fourier Transform.

**Obstacle vortex shedding phenomenon**

Vortices are formed due to changing pressure distribution along the surface of the propellant. The change in pressure distribution happens because of the obstacles created on the surface of the propellant (Yves Fabignon *et al.*, 2003; Hijlkema, 2011). The obstacle Vortices have been obtained for  $t_0+32$  s burning model for SRM-3. Fig.6 shows contour plot of vorticity magnitude with legend of the SRM-3 model. Fig.7 depicts the details of obstacle vortex shedding (VSO).

Fig.8. Pressure oscillations in SRM-3

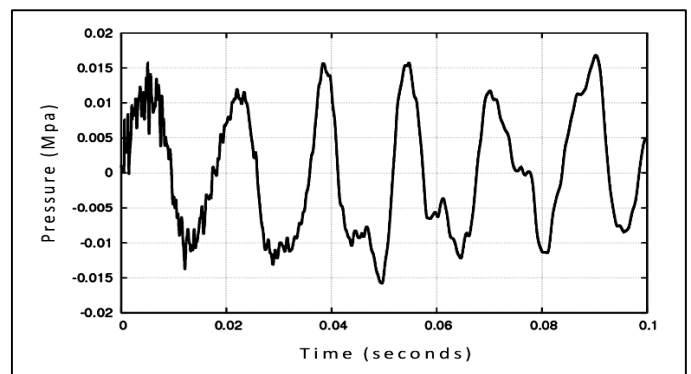


Fig.9. Frequency spectrum of pressure oscillations in SRM-3 obtained by CFD analysis

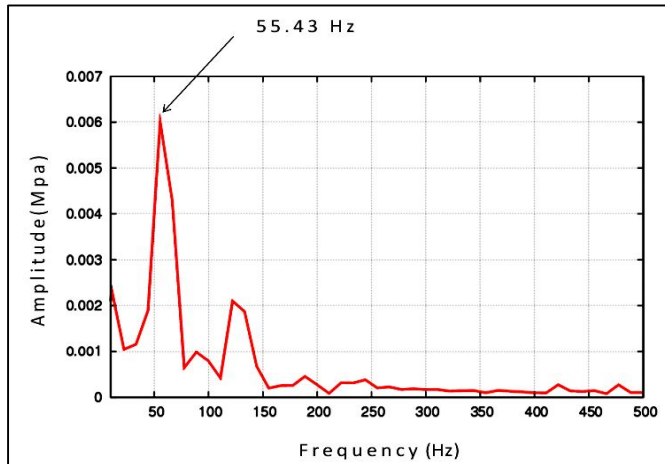


Fig.10. Frequency spectrum (3D plot) of pressure oscillations of SRM-3 during static test

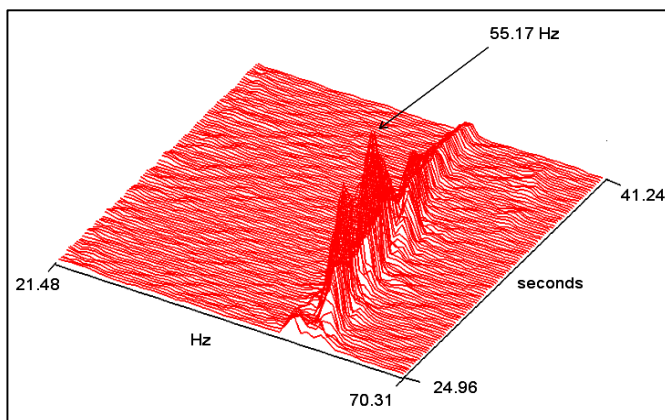
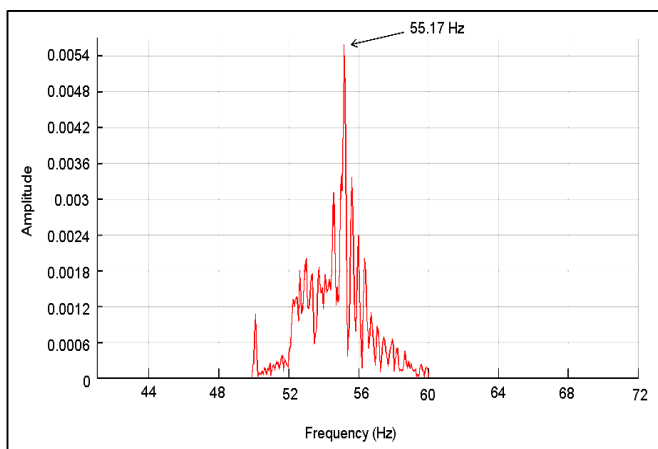


Fig.11. Frequency spectrum (2D plot) of pressure oscillations



**Processing of monitored data**

The magnified pressure - Time response plot for  $t_0+32s$  burning model is shown in Fig.8. The Pressure - Time data from the output of flow has been analyzed using the FLUENT software. The Amplitude - Frequency 2D plot obtained by analysis using FLUENT is shown in Fig.9. From these analyses, it is seen that the dominating frequency of oscillation (Obstacle Vortex Shedding) is 55.43Hz. Fig.10 depicts 3D plot of actual frequency spectrum of pressure oscillations observed during static test of SRM-3 and Fig.11 shows the same frequency spectrum in 2D plot.

**Results and discussions**

A validation setup has been conducted. Comparison of results of experimental data with the results of numerical simulation is also carried out to assess the reliability of the CFD analysis. From the comparison, it has been found that the result from experimental data closely matches with the analysis results. The frequency spectrum obtained by the analysis of the experimental data is peaking at 55.17Hz (Frequency Analysis Report, SFC, 2005) and the frequency spectrum obtained by numerical method is peaking at 55.43 Hz. It is worthy to note that this small difference is within the error band of the numerical simulation and the frequency resolution of the CFD analysis which are derived from the time step and the number of samples taken.

**Conclusions**

The static test result of SRM-3 has revealed unanticipated small amplitude pressure oscillations for certain duration of burning. Frequency spectrum of experimental data indicated peaking frequency of 55.17 Hz. Commercially available CFD software 'FLUENT' has been used to analyze the experimental data at the time of 32 s after ignition. This numerical analysis revealed occurring of Obstacle Vortex Shedding phenomena at the frequency of 55.43 Hz due to the compartmentalization of the combustion chamber by the protrusion of inhibition from the burning propellant surface at the segment joints. The results of the CFD analysis are found closely matching with the frequency of pressure oscillations within the accuracy of numerical analysis.

It is therefore concluded that the obstacle vortex shedding has most probably caused the pressure oscillations during the static test of SRM-3 motor.

To avoid this vortex shedding, it is suggested to optimize the thickness of the inhibition at the segment joints of SRM-3 so that the char and erosion rate of inhibition is more or less matches with the burn rate of the propellant thus formation of inhibition wall protruding from the burning propellant surface is minimal. Optimization of thickness of inhibition at the segment joints involves considerable experimentation at smaller scale models. This is proposed as future scope of work.



### Acknowledgement

The authors are grateful to Dr. R.K. Gupta and colleagues of Advanced Systems Laboratory, Hyderabad, Vice-Chancellor, Dr. M.G.R. Educational and Research Institute University for their kind help and support.

### References

1. Abdul Raheem S and Babu V (2004) Numerical simulations of unsteady flows in Solid Rocket Motors. *AIAA* 2004-2878, pp: 1-15.
2. Anonymous (2005) Post Test Inspection Report of SRM-3. SF Complex, DRDO, Jagdalpur (Confidential).
3. Anonymous (2005) Static Test Report of SRM-3. SF Complex, DRDO, Jagdalpur (Confidential).
4. Anonymous (2005) Test plan of SRM-3. ASL, DRDO, Hyderabad (Confidential).
5. Anonymous (2006) Frequency Analysis Report of SRM-3. SF Complex, DRDO, Jagdalpur (confidential).
6. David R Greatrix (2008) Transient burning rate model for solid rocket motor internal ballistic simulations. *Int. J. Aerospace Engg.* (826070), pp: 1-10.
7. Dotson KW, Koshigoe S and Pace KK (1997) Vortex shedding in large solid rocket motor without inhibitors at the segment interfaces. *J. Propulsion & Power.* 13(2), pp: 197-206.
8. Fluent (2006) 8.4.2 Viscosity as a function of temperature. Documentation FluentInc.
9. Hijlkema J, Prevost M and Cascalis G (2011) On the importance of reduced scale Ariane 5 P230 solid rocket motor models in the comprehension and prevention of thrust oscillations. *CEAS Space J.* 10<sup>th</sup> July, pp:99-107.
10. Price EW (1977) Combustion instability in solid rocket motors: Volume I- Executive summary, chemical propulsion information agency. *The Johns Hopkins University, CPIA Publ.*, 290, Nov.1, pp:4-5.
11. Robert S Brown, Roger Dunlap and Sunnyvale (1988) Acoustics oscillatory pressure control for solid propellant rocket. *Patent Number:* 4,765, 134, Aug.23, pp:2-4.
12. Scippa S, Pascal P and Zainer F (1994) Ariane-5 MPS: Chamber pressure oscillations full scale firing results analysis and further studies. *AIAA paper*94-3068 - 1994
13. Stella F and Paglia F (2009) Pressure oscillations in solid rocket motors: Effect of nozzle cavity. *J. Aerospace Sci., Technol. & Systems. Aerotechnica.* 88 (1/2 January -June) pp:31.
14. Stella F, Paglia F, Giangi M and Telara M (2005) Numerical simulation of pressure oscillations in solid rocket motors. *Eur. Conf. Aerospace Sciences (EUCASS) Moscow*, 5<sup>th</sup> July, pp: 1-8.
15. Tom Nesman and Eric Stewart (1996) RSRM Chamber pressure oscillations: Transit Time Models

and unsteady CFD. NASA, Marshall space flight center, AL 35812, pp: 1169-1187.

16. Yves Fabignon, Joel Dupays, Gerard Avalon, Francois Vuillot, Nicolas Lupoglazoff, Grégoire Casalis and Michel Prévost (2003) Instabilities and pressure oscillations in solid rocket motors. *Aerospace & Technol.* 7, pp: 191-200.